

Numerical calculation of thermal field and heat transfer coefficient for 160 kA aluminum reduction cell^①

FENG Nai-xiang(冯乃祥)¹, LIANG Fang-hui(梁芳惠)¹, SUN Yang(孙阳)¹,
PENG Jian-ping(彭建平)¹, LENG Zheng-xu(冷正旭)², XIE Qing-song(谢青松)²

(1. School of Materials and Metallurgy, Northeastern University, Shenyang 110004, China;
2. Guizhou Aluminum Smelter, Guiyang 550014, China)

Abstract The principle of thermal flux being constant in heat-flow-tube and the principle of heat balance were applied to analyze and calculate the steady-state thermal field and the electrolyte-ledge heat transfer coefficient of aluminum reduction cell by finite element method. The calculated results show that the melt-ledge heat transfer coefficient in the 160kA pre-baked anode aluminum reduction cell of Guizhou Aluminum Smelter is higher than that of other cells of the same current. It is also found that the electrolyte and metal flow much faster, which may be the results of poor bus bar arrangements. Meanwhile, the calculated results of melt-ledge heat transfer coefficient by heat-flow-tube method are almost in full agreement with the former works. This verifies the applicability of this method.

Key words: aluminum reduction cell; heat-current-tube; finite element method; heat transfer; heat balance

CLC number: TF 801.2

Document code: A

1 INTRODUCTION

The technologies of the 160 kA prebaked anode aluminum reduction cell of Guizhou Aluminum Smelter, China, were introduced from Japan in the 1970's. It has been found in the real operation that the target indexes are not as good as expected. For example, the current efficiency is lower than 88% and the DC power consumption for producing Al is higher than 14 000 kWh/t. Meanwhile, because of the bigger side channel, side ledge cannot be fully formed. It is analyzed that poor bus bar arrangements and inner lining structure as well as operation all have contributed to irregular ledge profile.

It is well known that the ledge profile is affected by the cell's lining structure, electrolyte temperature and its composition and melt-ledge heat transfer coefficient. For a cell with advanced bus bar arrangements and inner lining structure, its thermal field is much likely to be well distributed, the flow rates of electrolyte and metal will be lower, and so is the melt-ledge heat transfer coefficient. Besides these, metal height affects the melt-ledge heat transfer coefficient too, because metal height influences the thermal field and the flow rate of the metal.

Thermal field and thermal balance in the cell are important to maintain normal operation with higher current efficiency. Because the heat exchange of melt-ledge plays an important role in forming a reasonable and stable ledge^[1-5], it is rather significant to analyze

the melt-ledge heat transfer coefficient. In this paper, the finite element method is used to calculate the thermal field in the cell. Based on this calculation, heat-current-tube principle is applied to calculate the melt-ledge heat transfer coefficient. The pot structure and technological parameters of this kind of 160 kA prebaked anode aluminum reduction cell are listed in Table 1, and the bus bar arrangement is shown in Fig. 1.

Table 1 Pot structure and technological parameters of 160kA prebaked anode aluminum reduction cell

	Parameter	Value
Side structure	Side refractory brick	0.065 m
	Side carbon	0.060 m
	Depth of pot	0.460 m
Bottom structure	Width of side channel	0.525 m
	Calcium silicate board	0.065 m
	Alumina powder	0.025 m
	Insulating brick	0.130 m
Technological parameters	Refractory brick	0.130 m
	Cathode block	0.450 m
	Current	160 kA
	Cell voltage	4.03 V
	Anode current density	0.721 5 A/m ²
	Current supply	Bipolar
	Bath ratio	2.7-2.8
	Current efficiency	86%-87%

① Received date: 2002-05-29; Accepted date: 2002-11-27

Correspondence: FENG Nai-xiang, Professor; Tel: +86-24-83682562; E-mail: FENGNAIXIANG@163.com

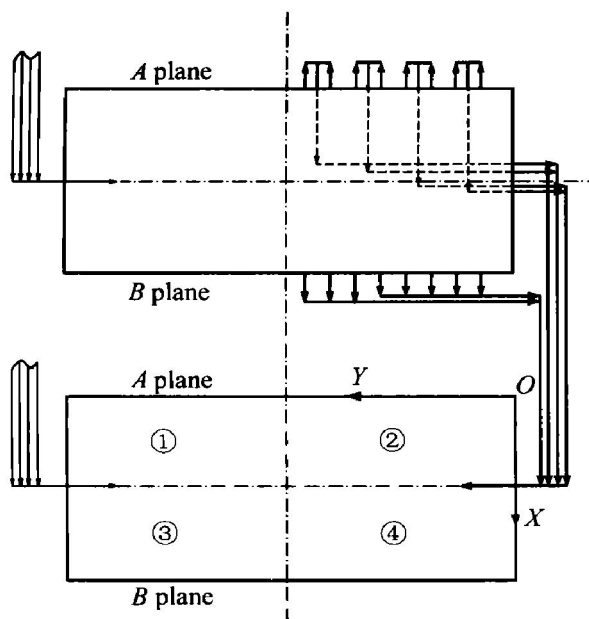


Fig. 1 Diagrammatic sketch of bus bar configuration of 160 kA prebaked anode aluminum reduction cell

2 CALCULATION OF THERMAL FIELD

2.1 Control equation of heat exchange and its boundary conditions

The control equation of 2-D steady-state heat exchange in the cell can be expressed as follows:

$$\frac{\lambda}{\rho c_p} \cdot \left[\frac{\partial^2 T}{\partial x^2} + \frac{\partial^2 T}{\partial y^2} \right] + \frac{q}{\rho c_p} = 0 \quad (1)$$

where λ is thermal conductivity, $\text{W}/(\text{m} \cdot \text{K})$; c_p is specific heat capacity at constant pressure, $\text{J}/(\text{kg} \cdot \text{K})$; ρ is density of material, kg/m^3 ; T is temperature, K ; q is heat produced within unit volume, J/m^3 .

The boundary conditions of the thermal field mathematical model in the aluminum reduction cell are described as follows.

On the interface touched with electrolyte, the first kind of boundary condition is adopted, namely the temperatures of the nodes on the interface equal the liquidus temperature of the electrolyte. On the surface of cathode carbon, the first kind of boundary condition is adopted too, namely the temperatures of the nodes on the surface of cathode equal that of the liquid aluminum. Because of symmetry, on the central symmetrical surface, the thermal insulation boundary condition is adopted. On the interface between anode and ledge and the top crust, the thermal insulation boundary condition is also adopted. Since the heat is emitted through the shell exterior surface by convection and radiation, where the third kind of boundary condition is adopted, the total heat transfer coefficient α can be calculated by the following equation:

$$\alpha = \alpha_c + \alpha_r = \alpha_c + \sigma_b (T_w^2 + T_f^2) (T_w + T_f) \quad (2)$$

where α_c is the convection heat transfer coefficient, $\text{W}/(\text{m}^2 \cdot \text{K})$; α_r is the radiation heat transfer coefficient, $\text{W}/(\text{m}^2 \cdot \text{K})$; σ_b is Steffer-Boltzmann constant, $\sigma_b = 5.67 \times 10^{-8} \text{ W}/(\text{m}^2 \cdot \text{K}^4)$; ε is the darkness of the shell surface; f is the angle coefficient; T_w and T_f are the shell surface and environment temperatures respectively, K .

2.2 Mesh division

The finite element meshes are shown in Fig. 2.

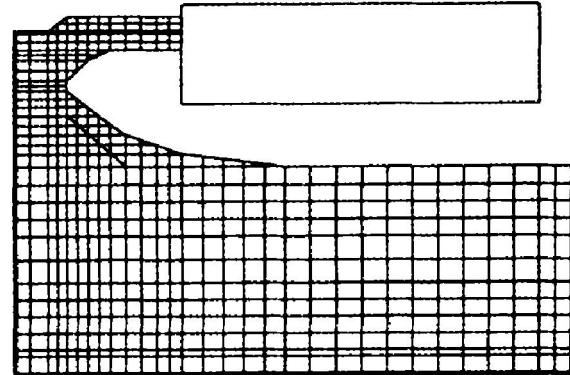


Fig. 2 Diagrammatic sketch of meshes in 160 kA prebaked anode aluminum reduction cell

After the area is meshed, variational calculation is done to calculate the heat exchange for every element by solving control equation under variational principle. Hence, the stiffness matrix of every element is got, so is the total stiffness matrix by synthesis. By solving the total stiffness matrix, the thermal field is obtained.

3 CALCULATION PRINCIPLE OF MELT LEDGE HEAT TRANSFER COEFFICIENT

In the course of heat transfer, heat flow line is conjugate with isothermal line which is vertical to the direction of heat transfer. The distribution of heat flow line in the cell is radial, as shown in Fig. 3.

Because the heat transfer is done along the heat flow line, the heat transfer does not take place at the both sides of the heat flow line, namely the heat flow line is a thermal insulation line. The adjacent two heat flow lines can form a heat-flow-tube. When the cell is at stable status, the heat flux through electrolyte bath and liquid aluminum is equal to that emitted to the environment by the shell. The total heat flux can be distributed into every heat-flow-tube, and in every heat-flow-tube, the thermal flux is constant (Fig. 4), so the following equation can be got:

$$Q_1 = Q_2 \quad (3)$$

where

$$Q_1 = \alpha_1 \cdot S_1 \cdot (T_{w1} - T_{f1}) \quad (4)$$

$$Q_2 = \alpha_2 \cdot S_2 \cdot (T_{w2} - T_{f2})$$

where Q_1 and Q_2 are the thermal fluxes entering

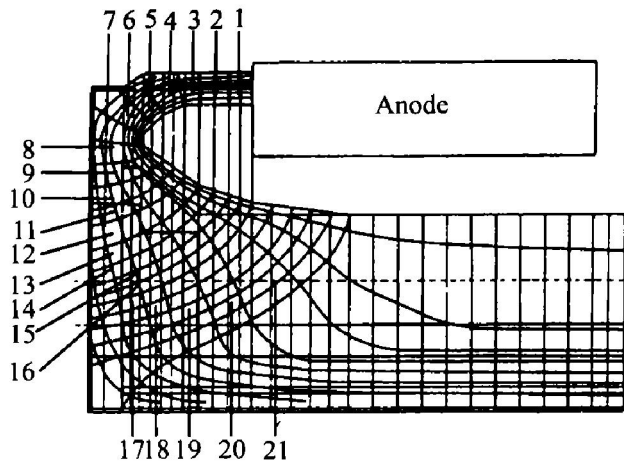


Fig. 3 Diagrammatic sketch of heat-flow-tube distribution in 160 kA prebaked anode aluminum reduction cell

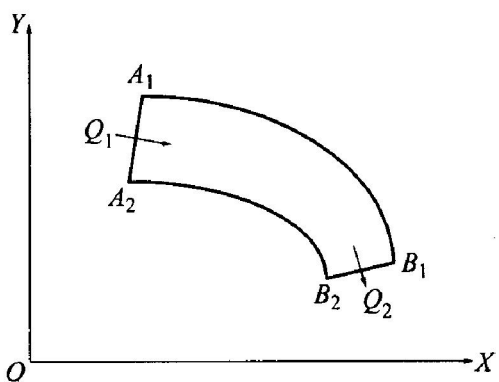


Fig. 4 Diagrammatic sketch of thermal flux in heat-flow-tube

and leaving heat-flow-tube, W ; α_1 and α_2 are the heat transfer coefficients on the surface of A_1A_2 and B_1B_2 , $W/(m^2 \cdot K)$; S_1 and S_2 are the areas of A_1A_2 and B_1B_2 , m^2 ; T_{w1} and T_{f1} are the temperatures of both sides of A_1A_2 surface, K ; T_{w2} and T_{f2} are the temperatures of both sides of B_1B_2 surface, K .

Taking the unit length as the thickness which is vertical to $X-Y$ plane, there is

$$S_1 = 1 \times A_1A_2, \quad S_2 = 1 \times B_1B_2 \quad (5)$$

From Eqns. (3), (4) and (5), one can get

$$\alpha_1 = \frac{\alpha_2 \cdot B_1B_2 \cdot (T_{w2} - T_{f2})}{A_1A_2 \cdot (T_{w1} - T_{f1})} \quad (6)$$

α_2 can be calculated from Eqn. (2). With Eqn. (6), the melt-ledge heat transfer coefficient α_1 can be calculated.

4 CALCULATION PRINCIPLE AND METHOD FOR EFFECT OF CELL VOLTAGE AND CURRENT CHANGE ON HEAT BALANCE

To begin with, the following definition is made: I is the current of the potline, ΔV is the cell voltage increase, namely, when the electrolyte bath voltage

increases ΔV , the heat produced within unit time increases $\Delta V \times I$. After a period of time, a new heat balance is reached. The delivery heat quantity within unit time increases ΔQ , which will be delivered through the shell surface, so the following equation can be got:

$$\begin{aligned} \Delta Q &= \Delta V \times I \\ &= \alpha(t_2 - t_0)S - \alpha(t_1 - t_0)S \end{aligned} \quad (7)$$

where α is the heat transfer coefficient between the shell and environment; t_0 is the environmental temperature; t_1 is the shell surface temperature before the voltage change; t_2 is the shell surface temperature after the voltage change; S is the delivery heat area of the shell.

$$t_2 = t_1 + \Delta t \quad (8)$$

where Δt is the temperature change on the shell surface.

Let δ_1 and δ_2 be the ledge thickness before and after the voltage change, $\Delta\delta$ be the ledge thickness change, so $\Delta\delta = \delta_1 - \delta_2$, and the following equation can be got, too:

$$I \times \Delta V = \frac{S \cdot (T' - t_2)}{\frac{l_1}{\lambda_1} + \dots + \frac{l_e}{\lambda_e}} - \frac{S \cdot (T - t_1)}{\frac{l_1}{\lambda_1} + \dots + \frac{l_e}{\lambda_e}} \quad (9)$$

where T' is the electrolysis temperature after the voltage change; T is the electrolysis temperature before the voltage change; l_1, \dots are the material thickness of the heat flux passing through; $\lambda_1 \dots$ are the thermal conductivities of materials; λ_e is thermal conductivity of the ledge.

The molar bath ratios will be increased after the ledge is melted. Since the total electrolyte quantity w and molar ratios are known before the ledge is melted, and if the molten electrolyte quantity is Δw , the electrolyte molar ratios is x_2 , and the liquidus temperature increase of the electrolyte ΔT can be calculated and got after the ledged is melted. If T_0 is the liquidus temperature before the voltage change and T'_0 is that after the voltage change, and the electrolysis temperature is 15 °C higher than the liquidus temperature, then these following equations can be got:

$$T = T_0 + 10; \quad T = T'_0 + 15 \quad (10)$$

$$\Delta T = T'_0 - T_0 = T' - T \quad (11)$$

In other words, after the voltage increase, the electrolysis temperature's increase is equal to the liquidus temperature's increase. The following equation can be got from Eqn. (11):

$$T' = T + \Delta T \quad (12)$$

Substitute Eqn. (12) into Eqn. (9), the following equation can be got:

$$I \times \Delta V = \frac{S \cdot (T + \Delta T - t_2)}{\frac{l_1}{\lambda_1} + \dots + \frac{l_e}{\lambda_e} - \frac{\Delta\delta}{\lambda_e}} - \frac{S \cdot (T - t_1)}{\frac{l_1}{\lambda_1} + \dots + \frac{l_e}{\lambda_e}} \quad (13)$$

Δw can be determined by the following equa-

tion:

$$\Delta w = d_c \cdot A_c \cdot \Delta \delta \quad (14)$$

where d_c is the ledge's density, kg/m^3 ; A_c is the ledge's area, m^2 . Because bath ratio change is the function of ledge melting thickness $\Delta \delta$, and the liquidus temperature's increase ΔT is also the function of $\Delta \delta$, thus

$$\Delta T = f(\Delta \delta) \quad (15)$$

By substituting Eqn. (15) to Eqn. (13), $\Delta \delta$ can be calculated.

In the course of actual calculation, reverse calculation method is taken. First, suppose ledge melting thickness is $\Delta \delta$ under the condition of cell voltage change ΔV , so the new electrolysis temperature can be worked out. Then the thermal field calculation program is used to calculate the cell shell's surface temperature, and the delivery heat quantity addition ΔQ will be obtained, too, which is equal to the heat increase generated due to cell voltage increase ΔV . So after cell voltage change, the change of ledge thickness can be determined. When there is current change, the calculation method is the same as above.

5 CALCULATED RESULTS AND DISCUSSION

5.1 Thermal field distribution

The thermal field distribution of 160 kA pre-baked anode aluminum reduction cell is shown in Fig. 5.

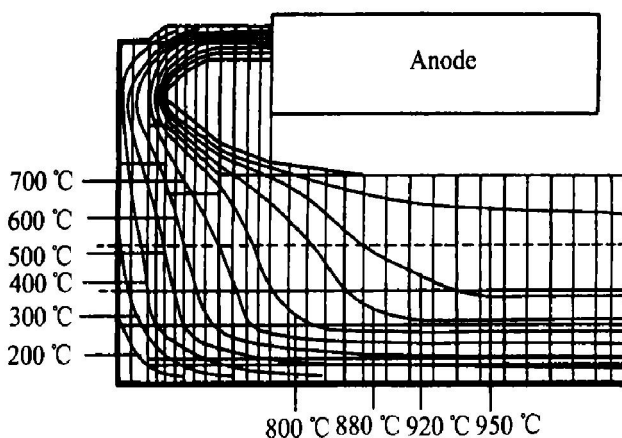


Fig. 5 Isothermal chart of thermal field in 160 kA prebaked anode aluminum reduction cell

(Temperatures of isothermal lines are 200, 300, 400, 500, 600, 700, 800, 880, 920, 950 °C from bottom to top)

From Fig. 5, it can be seen that at top crust and side ledge, isothermal line density is higher, so the temperature gradient is higher. At the inner lining structure of the cell bottom, the temperature gradient in the heat insulating material under the collector bar is higher. The refractory brick under the cathode carbon has higher temperature, above 900 °C, so electrolyte can be deposited on the cathode carbon surface easily, which results in the early breakage of cathode

carbon and short cell life.

5.2 Melt-ledge heat transfer coefficient

The melt-ledge heat transfer coefficient is shown in Table 2.

Table 2 Melt-ledge heat transfer coefficients

Heat-flow-tube No	Heat transfer coefficient ($\text{Wm}^{-2}\text{K}^{-1}$)	Heat-flow-tube No.	Heat transfer coefficient ($\text{Wm}^{-2}\text{K}^{-1}$)
1	146.25	12	614.35
2	153.35	13	601.01
3	188.85	14	600.62
4	191.54	15	527.65
5	508.14	16	460.90
6	1047.44	17	445.92
7	1 074.44	18	429.27
8	1 060.79	19	394.23
9	1 007.27	20	365.69
10	765.34	21	358.97
11	622.64		

From Table 2, it can be seen that the heat transfer coefficient is smaller on the top crust and bottom crust, while at the side ledge, the heat transfer coefficient is very high, about $1000 \text{ W}/(\text{m}^2 \cdot \text{K})$. The melt-ledge heat transfer coefficient given in lots of literatures is $500 - 1000 \text{ W}/(\text{m}^2 \cdot \text{K})$ ^[6, 7], so the calculated results are reasonable. But in this paper, the max melt-ledge heat transfer coefficient is about $1000 \text{ W}/(\text{m}^2 \cdot \text{K})$, which is much higher than that of other cells of same size, about $600 \text{ W}/(\text{m}^2 \cdot \text{K})$. Perhaps, it is the reason that the bus bar arrangements is not reasonable and that the vertical magnetic induction intensity is higher. This explanation had been verified by the magnetic field calculation and measurement, as well as the study on the liquid aluminum flow field^[8-10]. Compared with other same size cells, the current efficiency of the cell calculated in this paper is lower, which may be the result of higher fluid-ledge heat transfer coefficient.

6 CONCLUSIONS

The finite element method and the principle of the thermal flux being constant in heat-flow-tube are taken to calculate the steady-state thermal field and the melt-ledge heat transfer coefficient in 160 kA pre-baked anode aluminum reduction cell. It is shown that the melt-ledge heat transfer coefficient is higher in Guizhou Aluminum Smelter 160 kA prebaked an-

ode aluminum reduction cell. And it is also shown that the electrolyte bath and liquid aluminum flow much faster, which may mainly be caused by the unreasonable bus bar arrangements.

REFERENCES

- [1] QIU Zhuxian. Aluminum Electrolysis [M]. Beijing: Metallurgical Industry Press, 1982. (in Chinese)
- [2] Wittner H. How to influence the energy consumption figure by the ledge profile and metal pad[J]. Light Metals AIME, 1976: 49 - 56.
- [3] Haupin W E. Calculating thickness of containing walls frozen from melt[J]. Light Metals AIME, 1971: 188 - 193.
- [4] Fraser K J, Taylor M P, Jenkin A M. Electrolyte heat and mass transport processes in Hall-Heroult electrolysis cells[J]. Light Metals AIME, 1990: 221 - 226.
- [5] Bruggeman J N, Danka D J. Two-dimensional thermal modeling of the Hall-Heroult cell [J]. Light Metals AIME, 1990: 203 - 209.
- [6] Grjotheim K, Welch B. Aluminum Smelter Technology [M]. Dusseldorf: Aluminum-Verlag GmbH, 1988.
- [7] GUO Tianli. The Thermal Field Calculation of 160 kA Prebaked Anode Aluminum Reduction Cell [D]. Shenyang: Northeastern University, 1991.
- [8] SUN Yang, FENG Naixiang, LENG Zhengxu. Magnetic field measurement and calculation for 160 kA pre-bake cells in the Guizhou Aluminum Smelter[J]. Light Metals AIME, 2001: 433 - 437.
- [9] SUN Yang, FENG Naixiang, LENG Zhengxu. Numerical calculation of the effect of current distribution on the magnetic field inside a 160 kA aluminium reduction cell[J]. Light Metals, 2001(2): 30 - 33. (in Chinese)
- [10] FENG Naixiang, SUN Yang, LENG Zhengxu. Magnetic measurement and calculation of 160 kA prebake cell in Guizhou Aluminum Smelter[J]. Light Metals, 2000(11): 43 - 47. (in Chinese)

(Edited by YUAN Saiqian)